International Journal of Mass Spectrometry 306 (2011) 219–226

Contents lists available at ScienceDirect

International Journal of Mass Spectrometry

journal homepage: www.elsevier.com/locate/ijms

Sequential IRMPD of $XGe(OEt)_4^-$ ions: Gas-phase synthesis of novel oxy-germanium anions

Luciano A. Xavier[a], Thaciana V. Malaspina[b], Nelson H. Morgon[c], Jair J. Menegon[a], José M. Riveros[a,b,*]

[a] Instituto de Química, Universidade de São Paulo, Caixa Postal 26077, São Paulo CEP 05508-900, Brazil
[b] Centro de Ciências Naturais e Humanas, Universidade Federal do ABC, Santo André, SP, CEP 09210-270, Brazil
[c] Instituto de Química, Universidade Estadual de Campinas, Caixa Postal 6154, Campinas, SP, CEP 13083-970, Brazil

ARTICLE INFO

Article history:
Received 15 September 2010
Received in revised form
20 November 2010
Accepted 29 November 2010
Available online 13 December 2010

Keywords:
Germanium tetraethoxide
Pentacoordinated Ge anions
IRMPD
Germanate anions
Germyl anions

ABSTRACT

The gas-phase ion/molecule reactions of F^- and EtO^- with $Ge(OEt)_4$ yield readily and exclusively pentacoordinated complexes $XGe(OEt)_4^-$ (X = F, EtO) at pressures in the 10^{-8} T range as observed by FT-ICR techniques. These hypervalent species are prone to undergo sequential fragmentations induced by infrared multiphoton excitation that lead to a variety of germyl and germanate anions. In the case of $FGe(OEt)_4^-$, three primary competitive channels are observed in the IRMPD process that can be identified as $(EtO)_3GeO^-$, $F(EtO)_2GeO^-$ and $(EtO)_3Ge^-$. Ab initio calculations have been carried out to characterize the primary fragmentation paths induced by IRMPD and the most favorable structure of the resulting anions. The gas-phase acidity of a number of these germanium-containing ions have been estimated by bracketing experiments and by theoretical calculations. Germanate anions such as $(EtO)_3GeO^-$ undergo some interesting reactions with H_2S to give rise to anions such as $(EtO)_3GeS^-$ and $(EtO)_2Ge(OH)S^-$.

1. Introduction

The gas-phase ion chemistry of organo-germanium compounds remains relatively unexplored [1]. Thermochemical properties for simple Ge-containing ions are scarce when compared with their silicon analogs [2] and even bond energies are poorly characterized [3]. Yet, simple germanium compounds play an important role in chemical vapor deposition processes [4] and in sol–gel processes [5] used for the synthesis of advanced materials [6]. A particularly useful reagent for these purposes is the family of homoleptic germanium alkoxides, $Ge(OR)_4$, that have been used in the preparation of important materials such as GeS_2 [7], Ge-containing nanoparticles [8,9] as well as for deposition of germanium dioxide [10] and organogermanium films [11].

The variety of applications found for these alkoxides has motivated studies aimed at understanding the chemical reactions relevant to sol–gel processes and chemical vapor deposition. Germanium alkoxides, similar to other metal alkoxides, are prone to undergo hydrolysis followed by extensive polycondensation reactions [12,13]. The mechanism describing the early stages of the hydrolysis reactions has been addressed in a recent report [14] but the characterization of possible transient oxy-germanium intermediate species remains elusive because of the complexity of the processes [15]. The structure and bonding of some simple germanium oxyhydroxides have been characterized theoretically [16] but finding ways to prepare and characterize oxy-germanium intermediate species is still a challenging proposition.

One approach that can be used to elucidate the fundamentals of the underlying chemistry of oxy-germanium species involved in sol–gel reactions is to probe some of these processes by mass spectrometry. For example, attempts to elucidate mechanistic details of polycondensation processes in neat $Ge(OEt)_4$ and in $Ge(OEt)_4/Si(OEt)_4$ mixtures by gas-phase ion chemistry techniques were pioneered by Taldi and coworkers [17]. Likewise, electrospray ionization was used to observe the formation of mono- and oligo-germanium acids in the reaction of germanium ethoxide with HCl leading to the formation of germanium dioxide crystallites [18]. The structural elements of mixed Si/Ge zeolites have also been recently probed by electrospray ionization [19]. Our group has previously investigated the gas-phase positive ion chemistry of $Ge(OMe)_4$ [20] as well as the ion–molecule reactions of a number of anionic nucleophiles with the same neutral substrate [21]. In the latter study, reactions were shown to proceed almost exclusively by initial addition of the nucleophile to the Ge center to yield pentacoordinated anions.

The present report describes some of the anionic gas-phase ion chemistry of germanium ethoxide, $Ge(OEt)_4$ or TEOG, and the generation of oxy-germanium anions by sequential infrared mul-

* Corresponding author at: Institute of Chemistry, University of São Paulo, Av. Lineu Prestes 748, Cidade Universitária, São Paulo 05508-900, Brazil.
Tel.: +55 11 3091 3888; fax: +55 11 3091 3888.
E-mail address: jmrnigra@quim.iq.usp.br (J.M. Riveros).

1387-3806/$ – see front matter © 2010 Elsevier B.V. All rights reserved.
doi:10.1016/j.ijms.2010.11.019

tiphoton dissociation of hypervalent anionic adducts of TEOG. The likely structures of these novel oxy-germanium species have been determined by computational chemistry, and their proton affinities estimated from a combination of bracketing experiments and theoretical calculations.

2. Experimental

Experiments were carried out in our custom made FT-ICR spectrometer interfaced to an IonSpec Omega Fourier Transform Data System [22]. The spectrometer is based on a water cooled 9" electromagnet that is normally operated at 1.0 T, and contains a ~15.6 cm^3 cubic cell with center holes drilled on both transmitter plates to allow for laser light to go through the cell. The vacuum chamber housing the ICR cell is provided with two opposing ZnSe windows that act as entry and exit ports for infrared laser radiation.

Fluoride ions were generated by electron impact from NF_3 (Air Products) with 90 ms pulses at pressures around 3×10^{-8} T (ion gauge reading). The electron energy was maintained at 3 eV and the trapping voltage at −1.9 V. A radio-frequency field of ~7 MHz was applied to one of the trapping plates during ~140 ms to eject trapped thermal electrons from the cell. Fresh samples of germanium ethoxide, $Ge(OEt)_4$, (Strem Chemicals, 99.99 + %-Ge) were thoroughly degassed by repeated freeze–pump–thaw cycles, and purified by distilling off *in situ* any volatile residues produced by hydrolysis of the sample [23]. The typical partial pressures of TEOG used in this work were in the range of $2–5 \times 10^{-8}$ T. Under these conditions, the fluoride ions react completely in less than 2 s. Similar experiments were also carried out using EtO^- and MeO^-, generated from the corresponding alkyl nitrites, as the nucleophile reagents.

The infrared photodissociation experiments (IRMPD) were carried out after selective isolation of the ion of interest. All unwanted ions were ejected with a combination of short (2 ms) on-resonance radiofrequency (RF) bursts, and long RF sweeps (10–15 ms) over a wide mass range. In the case of the stepwise photodissociation experiments, each of the primary photoproducts was individually re-isolated after 200–500 ms of irradiation time. A grating tunable cw CO_2 laser (SYNRAD, Model 48G-1) was used as the infrared source in the multiphoton dissociation experiments. The laser was operated on the P(30) line of the 9.6 μm band at 1037 cm^{-1} for the experiments involving the germanium-containing ions. The power level of the laser was externally controlled by varying the width of a 10 kHz modulation pulse from a Hewlett–Packard pulse generator. The laser power measured at the exit window of the vacuum system of the spectrometer was typically 1–3 W. The irradiation time was controlled by an electro-mechanical shutter placed in front of the laser, whereas the trigger and aperture times of the shutter were determined by a pulse from the IonSpec Data System. Sequential IRMPD can be studied conveniently with this arrangement by using several pulses programmed for different delay times. This arrangement is similar to a procedure previously described in the literature [24].

Collisionally activated dissociation experiments by sustained off-resonance irradiation (CAD-SORI) [25] were also carried out to characterize the primary dissociation products of $FGe(OEt)_4^-$. For these experiments, the irradiation frequency was typically set at 200 Hz above the resonant frequency of the selected $F^{74}Ge(OEt)_4^-$ species and complete dissociation could be achieved with less than 500 ms irradiation time.

The proton affinity of some of the fragment ions obtained from IRMPD was estimated by bracketing-type experiments. The anions of interest were isolated after formation by IRMPD and neutrals of well-known gas-phase acidity were introduced through a pulsed valve with typical pulse widths in the range of 10–15 ms. Spectra were collected after a suitable delay time of 200–300 ms after activation of the pulsed valve, and a delay time of 25 s was used between sets of spectral accumulation to allow for return to the original base pressure in the cell.

All other reagents were obtained commercially and subjected to several freeze–pump–thaw cycles before sample introduction.

3. Computational details

Calculations were carried out with the Gaussian 03 suite of programs [26]. Two different sets of methodologies were used to obtain the structures and energies for neutral and anionic species containing germanium. The first approach consisted initially of pre-optimizing the structures at the HF/3-21G and these structures used as input for a new set of optimization calculations at the B3LYP/6-311++G(d,p) basis set. The final energies were then evaluated for the final optimized geometry. All degrees of freedom were optimized, and only positive vibrational frequencies were obtained at these optimized geometries at the B3LYP/6-311++G(d,p) level. The final thermochemistry for reactions and relative order of stability of isomeric structures were obtained by correcting all vibrational frequencies by scale factor of 0.9613 suggested by Andersson and Uvdal [27].

The second approach made use of the general procedure outlined in our earlier studies of the electron affinity of simple germyl radicals [28] and of anionic hypervalent complexes of Ge [29]. These calculations were carried out at the QCISD(T) level using a pseudopotential for the internal electrons and included diffuse and polarization functions for the outer electrons and for convenience are identified as the B1 basis set. The zero point energies (ZPE) were calculated from vibrational frequencies obtained from structures optimized at the Hartree–Fock level with the same basis set (HF/B1).

A detailed comparison of theoretical methods was not carried out at this point because it was outside the scope of our work. However, the results described below suggest that comparisons between these methods should be explored in the future.

4. Results and discussion

4.1. Ion–molecule reactions

F^- reacts readily with $Ge(OEt)_4$ under our experimental conditions to yield an adduct ion as shown in reaction (1).

$$F^- + Ge(OEt)_4 \rightarrow [FGe(OEt)_4]^- \quad (1)$$

The FT-ICR spectrum obtained after 1 s of reaction displays the typical cluster of different Ge isotopes with the base peak at *m/z* 273 corresponding to the most abundant ^{74}Ge isotopologue. Unlike the reaction of F^- with $Ge(OMe)_4$ [21], no other reaction products were detected in this case.

A somewhat similar behavior was observed when EtO^- was used as the nucleophile (reaction (2)). Reaction (2b) could also be observed in experiments where the reactant EtO^- ions are not properly thermalized before ion isolation.

$$EtO^- + Ge(OEt)_4 \rightarrow Ge(OEt)_5^- \quad (2a)$$

$$EtO^- + Ge(OEt)_4 \rightarrow (EtO)_3GeO^- + (EtOH + C_2H_4) \text{or} (EtOEt) \quad (2b)$$

The reaction of $Ge(OEt)_4$ with MeO^- results predominantly in displacement of EtO^-. In this case, formation of the hypervalent ion $MeOGe(OEt)_4^-$ becomes a minor reaction channel (<10%). In addition, other minor reaction products are observed along with the sequential reactions of EtO^- ions shown in reaction (2). The minor reaction products could be better characterized in experiments where EtO^- ions formed in reaction (3a) were continuously

ejected from the cell. The full set of reactions for the $MeO^-/Ge(OEt)_4$ system is shown below.

$$MeO^- + Ge(OEt)_4 \rightarrow EtO^- + MeOGe(OEt)_3 \quad > 90\% \quad (3a)$$

$$MeO^- + Ge(OEt)_4 \rightarrow [(EtO)_4GeOMe]^- \quad < 2.5\% \quad (3b)$$

$$MeO^- + Ge(OEt)_4 \rightarrow (EtO)_3Ge^- + EtOH + CH_2O \quad (or CH_3CHO + MeOH) \quad < 6\% \quad (3c)$$

$$MeO^- + Ge(OEt)_4 \rightarrow (EtO)_3GeO^- + MeOH + C_2H_4 \quad < 1\% \quad (3d)$$

$$MeO^- + Ge(OEt)_4 \rightarrow [MeOGe(H)(OEt)_3]^- + CH_3CHO \quad < 0.5\% \quad (3e)$$

Reactions (1)–(3) bear resemblance to those previously reported for the reaction of these same nucleophiles with $Ge(OMe)_4$ [21] with reactions proceeding initially by addition of the nucleophile to the Ge substrate. Because of the low abundance of the product ions as a result of reactions (3b)–(3e), these reactions were not studied in detail.

The most stable structure for the complex resulting from addition of F^- to $Ge(OEt)_4$ is shown in Fig. 1 as a typical example of a Ge pentacoordinated complex. The structure corresponds to a near trigonal bipyramid arrangement around the Ge center with the incoming fluorine sitting on an apical position in agreement with our previous calculations [21].

The calculated binding energies for the apical groups in $FGe(OEt)_4^-$ are shown in Eq. (4) because they are relevant in the discussion of the dissociation of the pentacoordinated complexes. Nevertheless, some caution is necessary with our calculated values because significant differences with experiment can be obtained using different methods and different basis sets for Ge systems of this type [30].

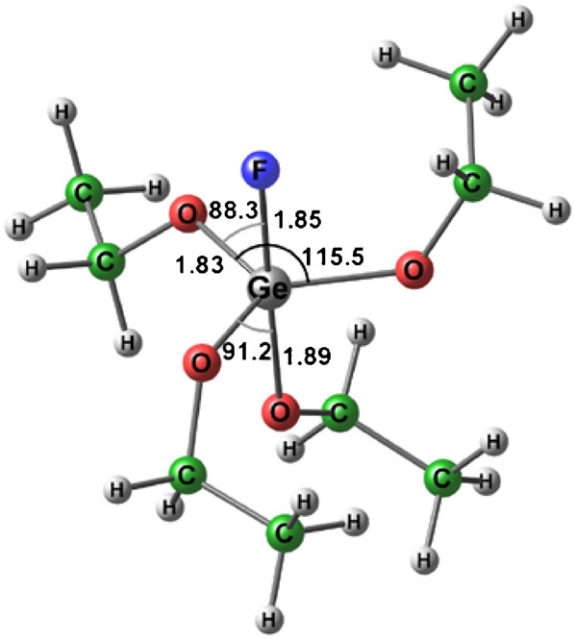

Fig. 1. Calculated structure for $FGe(OEt)_4^-$ at the B3LYP/6-311+G(d,p) level.

The nature of the neutral products has been assumed on the basis of the possible mechanisms for the dissociation processes (see below).

The occurrence of these three competing channels is very unusual for ions of this size. No noticeable difference in product distributions was found by varying the laser irradiation power in the range of 0.5–3.0 W. Furthermore, identical results were obtained from dissociation of $[FGe(OEt)_4]^-$ in SORI-CAD experiments.

By comparison, the IRMPD of $Ge(OEt)_5^-$ resulted in only one primary dissociation channel,

$$[FGe(OEt)_4]^- \rightarrow F^- + Ge(EtO)_4 \quad \Delta H(calc) = 49.2 \text{ kcal mol}^{-1} \quad (4a)$$

$$[FGe(OEt)_4]^- \rightarrow EtO^- + FGe(EtO)_3 \quad \Delta H(calc) = 49.9 \text{ kcal mol}^{-1} \quad (4b)$$

4.2. IRMPD of the $[XGe(OEt)_4]^-$ ions

As in our previous work with the hypervalent anionic adducts of $Ge(OMe)_4$ [20], the possibility of obtaining a variety of Ge-containing anions lead us to explore dissociation of activated $[XGe(OEt)_4]^-$ anions. The infrared spectrum of $Ge(OEt)_4$ exhibits a strong absorption at 1045 cm^{-1} [23] that was attributed to be a characteristic vibration of the GeO_4 moiety. The fact that this absorption coincides with the most intense P branch transitions of the CO_2 laser prompted us to study the IRMPD behavior of the $[XGe(OEt)_4]^-$ anions.

Extensive and sequential IRMPD processes are observed both for $[FGe(OEt)_4]^-$ and $Ge(OEt)_5^-$ in a manner reminiscent of that reported for gas-phase $FTi(O^iPr)_4^-$ adducts [22]. At short irradiation times (<100 ms), IRMPD of isolated $[FGe(OEt)_4]^-$ ions revealed three primary dissociation channels as shown in (5).

$$[F^{74}Ge(OEt)_4]^- + nh\upsilon_{IR} \rightarrow \begin{cases} \sim 39\% & (EtO)_3{}^{74}GeO^- \text{ (m/z 225)} + C_2H_4 + HF \quad (5a) \\ \sim 25\% & (EtO)_3{}^{74}Ge^- \text{ (m/z 209)} + CH_3CHO + HF \quad (5b) \\ \sim 36\% & F^{74}Ge(EtO)_2O^- \text{ (m/z 199)} + C_2H_4 + EtOH \quad (5c) \end{cases}$$

$$[^{74}Ge(OEt)_5]^- + nh\upsilon_{IR} \rightarrow (EtO)_3{}^{74}GeO^- (m/z225) + C_2H_4 + EtOH \quad (6)$$

Two possible mechanisms for the dissociation of vibrationally activated $Ge(OEt)_5^-$ are outlined in Scheme 1: (a) pathway A is envisioned to yield a nascent EtO^- that promotes an internal return reaction through an E2-type elimination reaction by abstraction of a β-hydrogen from one of the ethyl groups, or less likely by an S_N2 mechanism to yield diethyl ether; (b) pathway B is envisioned to proceed through a cyclic transition state with elimination of EtOH and C_2H_4.

Our experiments with $Ge(OEt)_5^-$ do not yield an unequivocal answer to which mechanism is more likely.

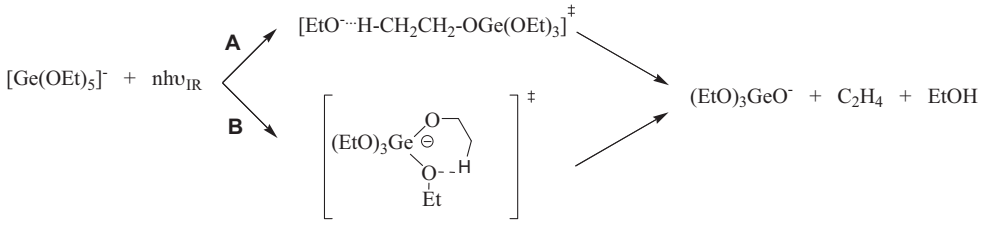

Scheme 1.

The results obtained for $[FGe(OEt)_4]^-$ provide us with some further information. The kinetics of photofragmentation of $[FGe(OEt)_4]^-$ were recorded by varying the aperture time of the shutter and the rate constant was measured to be $(3 \pm 0.5)\,s^{-1}$ at a laser power of 3 W. For $[FGe(OEt)_4]^-$ ions with 96 vibrational modes, the IRMPD process can still be considered to be in the slow energy exchange limit [31] and the rate of pumping likely to be the rate determining step. Thus, ignoring kinetic shifts for rate constants of this order of magnitude, the activation energies for reactions (5a)–(5c) should be comparable for the three dissociation channels in the absence of dramatic entropy effects.

The product distribution for reactions (5a)–(5c) bears no relationship with the calculated enthalpies for the reactions shown in Table 1 as might be expected for processes that do not involve simple bond cleavages

The possibility that processes (5a) and (5c) proceed by pathways similar to B (Scheme 1) was initially explored by theoretical calculations. However, transition states for either HF or EtOH elimination via a cyclic pathway (Scheme 1) could not be located in spite of several attempts using different methodologies. On the other hand, the almost identical dissociation energies calculated for F^- and EtO^- in Eq. (4) suggest that the competitive dissociation processes may occur from activated $[F^-–Ge(OEt)_4]$ or $[EtO^-\cdots(EtO)_3GeF]$ loose complexes that proceed by abstraction of a β-hydrogen, or in the latter complex additionally by H^- transfer to the Ge center followed by HF and CH_3CHO elimination. This last pathway was previously observed in the reaction of F^- with $Ge(OMe)_4$ where the hydride adduct $HGe(OMe)_4^-$ was in fact detected as one of the ion/molecule reaction products [21].

While the three competing processes observed in reaction (5) are unusual, the sequential IRMPD processes also proved to be of considerable interest.

4.3. IRMPD of $[Ge(OEt)_3]^-$ ions

Eq. (7) reveals the sequential IRMPD process observed for the $(EtO)_3Ge^-$ anions. These processes involve progressive H^- transfer presumably from a departing EtO^- group followed by H^- transfer to the Ge center.

$$(EtO)_3Ge^- \xrightarrow{IRMPD} CH_3CHO + (EtO)_2GeH^- \xrightarrow{IRMPD} CH_3CHO + EtOGeH_2^- \quad (7)$$

A possible third step leading to GeH_3^- was not observed but presumably it reflects a much slower process. These results are significant because it provides a route for generating germyl anions that are not easily generated and characterized in condensed phases [32] in spite of some useful synthetic applications [33].

Table 1
Calculated enthalpies for the dissociation processes of $FGe(OEt)_4^-$ at the B3LYP/6-311++G(d,p) level.

	Reaction (5a)	Reaction (5b)	Reaction (5c)
$\Delta H°$/kcal mol^{-1}	37.8	32.0	24.7

4.4. IRMPD of $F(EtO)_2GeO^-$ and $(EtO)_3GeO^-$ ions

Further IRMPD dissociation processes were also observed for the primary dissociation ion products of (5a) and (5c). These are shown below.

$$F(EtO)_2GeO^- \xrightarrow{IRMPD} EtOH + FGe(O_2C_2H_4)^- \quad (8)$$

$$(EtO)_3GeO^- \xrightarrow{IRMPD} EtOH + Ge(O_3C_4H_9)^- \xrightarrow{IRMPD} C_2H_4 + Ge(O_3C_2H_5)^- \quad (9)$$

Both germanates eliminate ethanol (or C_2H_4 and H_2O) in the secondary IRMPD process to yield anions whose structures are not obvious. Several possible isomeric species can be proposed for the $GeFO_2C_2H_4^-$ and $GeO_3C_4H_9^-$ species, that can be represented as either germyl or germanate structures. Four of these isomers are shown in Fig. 2 for $GeO_3C_4H_9^-$ along with the calculated relative energies. The germyl anion structures are more stable than the germanate anion structures with IIA, $EtOGe(OCH{=}CH_2)(OH)^-$, being the most stable isomer. Similar results are obtained for $GeFO_2C_2H_4^-$ with the $FGe(OCH{=}CH_2)(OH)^-$ being the most stable isomer. In general, the trend for Ge systems is that the germyl anion structures are more stable than the isomeric germanates as also calculated for model systems such as $(HO)_3Ge^-$ and $H(HO)_2GeO^-$, and $MeO(HO)_2Ge^-$ and $MeO(H)(HO)GeO^-$. The Ge anions with cyclic ligand structures were considered in view of the fact that these moieties have been previously characterized in the reactions of $Ge(OEt)_4$ with diols in solution [34].

The subsequent loss of C_2H_4 in the ternary photodissociation process is observed only for the $GeO_3C_4H_9^-$ ion (Eq. (9)) but not for the fluorine substituted Ge-containing anion, $GeFO_2C_2H_4^-$ (Eq. (8)). Based on the isomers shown in Fig. 2, four different isomers corresponding to germyl and germanate anions are shown in Fig. 3 for the $GeO_3C_2H_5^-$ ion produced in the ternary IRMPD process (Eq. (9)). The dihydroxygermyl anion, IIIA, is calculated to be the most stable species and considerably more stable than the isomeric germanates.

In spite of the preferred stability for the germyl anion structure, there is no simple mechanism to explain the formation of the germyl anion IIA and how IIA would then undergo ethylene elimination in Eq. (9). On the other hand, a tentative mechanism for the secondary IRMPD processes can be proposed based on the idea of a nascent EtO^-, from $(EtO)_3GeO^-$ (or from $FGe(OEt)_2O^-$ in Eq. (8)) promoting a proton abstraction from another ethoxy group to yield ethanol followed by ring closure to yield the IID germanate isomer (or the fluorine equivalent). The IID ion could then undergo ethylene elimination in the ternary IRMPD process by proton transfer to yield the IIIC germanate isomer. This putative pathway would explain the fact that no ternary IRMPD process occurs for the $FGe(O_2C_2H_4)^-$ ion where no ethoxy groups are available. This proposal takes into account the fact that species con-

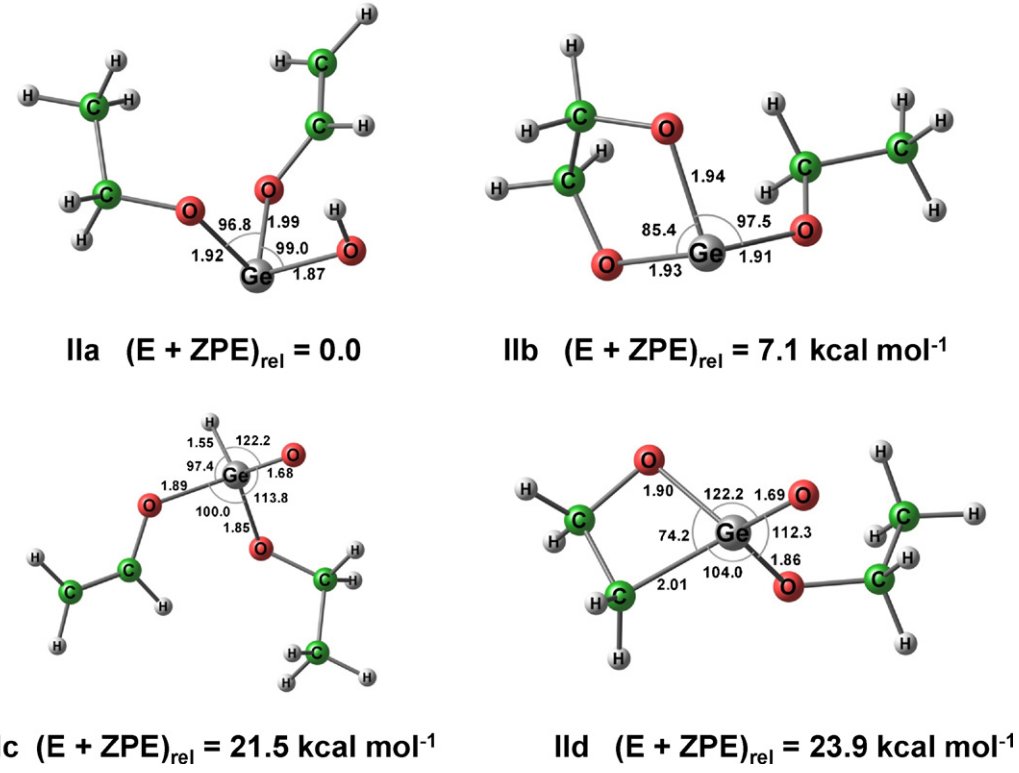

Fig. 2. Structures and relative energies of some of the $[Ge,O_3,C_4,H_9]^-$ isomeric ions calculated at the B3LYP/6-311+G(d,p) level.

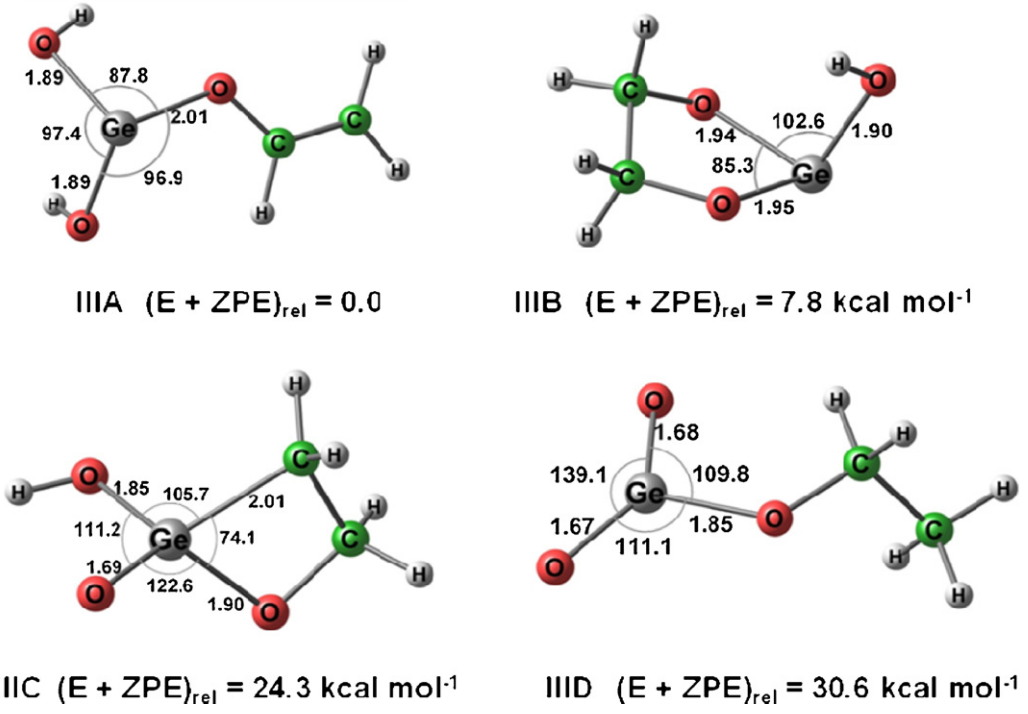

Fig. 3. Structures and relative energies of some of the $GeO_3C_2H_4^-$ isomeric ions calculated at the B3LYP/6-311+G(d,p) level.

taining a Ge=O group are notoriously unstable as illustrated for germanones [35,36].

The possibility of an isomerization of a germanate to a germyl anion was also explored for a model system. This process is illustrated in Fig. 4 for the isomerization of $(HO)_3Ge^-$ to $HGe(OH)_2O^-$ as an example of the energy barriers involved in this process. While the high energy calculated for the system may reflect some contribution from intramolecular hydrogen bonding, the results clearly indicate that isomerization between the two forms is unlikely in the time frame of an FT-ICR experiment. Some related isomerization processes for similar neutral Ge molecular systems also reveal substantial energy barriers [37].

Some of the proton transfer reactions described in Part 4.6 support the assignment of a germanate structure to the ions generated by IRMPD in Eqs. (8) and (9).

4.5. Reactivity and IRMPD behavior of $Si(OEt)_4$

Because similar gas-phase ion/molecule reactions have been previously reported [38,39] for the analogous silicon compounds, namely $Si(OMe)_4$ and $Si(OEt)_4$, it is interesting to compare similarities and differences with the behavior of the Ge substrates. The reaction of F^- with $Si(OEt)_4$ has been shown to proceed by initial formation of the hypervalent adduct $FSi(OEt)_4^-$ in a similar fashion to that described above for $Ge(OEt)_4$. However, under the low pressure conditions of FT-ICR experiments, displacement of EtO^- was also observed as a result of fragmentation of non-thermalized hypervalent siliconate species [38].

Comparative IRMPD experiments of $FSi(OEt)_4^-$ carried out under the same conditions to those used for $FGe(OEt)_4^-$ reveal two important differences: (a) considerably higher laser powers and longer irradiation times are needed to promote dissociation; (b) only one channel of dissociation is observed followed by sequential IRMPD processes, as shown in (10)

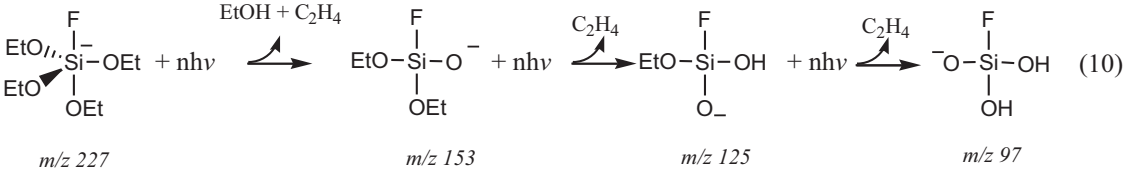

(10)

The first dissociation is similar to process (5c) and suggests that that the EtO^- affinity of $FSi(OEt)^-$ is less than the F^- affinity of $Si(OEt)_4$ [40]. However, the most noticeable difference resides in the fact that no hydride transfer to the metal center is observed that would result in loss of acetaldehyde as in (5b). This exact same behavior is observed for $FGe(OMe)_4^-$ [21] and $FSi(OMe)_4^-$ [38]. Thus, the Si and Ge substrates display important differences in the primary dissociation channels.

The subsequent IRMPD processes described in (10) are also different than those observed for the equivalent $FGe(OEt)_2O^-$ species in (8). The successive loss of olefin moieties from the silicate anions is not observed for the fluorgermanate anions, and resembles more than behavior observed in the sequential IRMPD processes of similar titanate anions (22).

4.6. Experimental and theoretical estimates of the proton affinities of germanates and germyl anions

The gas-phase acidities of germanic acid, $Ge(OH)_4$, and related germanols, X_3GeOH, are of particular interest because of the limited data available for these systems. In solution, $Ge(OH)_4$ is known to be a weak acid with a quoted pK_a value of 8.6 [41]. At around pH 10, the $(HO)_3GeO^-$ anion becomes the predominant species [42]. In the meantime, the gas-phase $\Delta_{acid}H^\circ$ at 298 K of $Ge(OH)_4$ has been calculated to be 348.4 kcal mol^{-1} at the G2 level [43] and provide an initial value for comparison. By comparison, the gas-phase $\Delta_{acid}H^\circ$ of GeH_4 has been determined experimentally to be 359.0 ± 1.3 kcal mol^{-1} [44]. Our previous calculations reveal that oxygen-containing substituents on Ge progressively decrease the value of $\Delta_{acid}H^\circ$. For example, the $\Delta_{acid}H^\circ$ of $MeOGeH_3$ was calculated to be 5 kcal mol^{-1} less than that of germane [28], whereas the $\Delta_{acid}H^\circ$ for $HGe(OH)_3$ was estimated to be 342 kcal mol^{-1} based on the heterolytic dissociation to yield $(HO)_3Ge^-$ and a proton [45]. Fluorine substituted germanes are predicted to be significantly more acidic than these model systems [28,45].

Table 2
Calculated $\Delta_{acid}H^\circ$ for a number of oxygen–germanium substrates.

Neutral	Anion	($\Delta_{acid}H^\circ$/kcal mol^{-1})[a]	($\Delta_{acid}H^\circ$/kcal mol^{-1})[b]
$HGe(OH)_3$	$(HO)_3Ge^-$	334.2	343
	$H(OH)_2GeO^-$	350.9	352
$H(OH)Ge(OMe)_2$	$(HO)(MeO)_2Ge^-$	333.4	340
	$H(MeO)_2GeO^-$	352.1	353
HF_2GeOH	$F_2(HO)Ge^-$	315.0	327
	HF_2GeO^-	338.5	344
$(EtO)_3GeOH$	$(EtO)_3GeO^-$	347.4	
$F(EtO)_2GeOH$	$F(EtO)_2GeO^-$	341.4	

[a] Values calculated at the B3LYP/6-311++G(d,p) level.
[b] Values obtained at the QCISD(T)/B1//HF/B1 level where B1 represents the basis set described in Ref. [28].

Experiments using a number of substrates of known gas-phase acidities [46] were used in an attempt to bracket the proton affinity of some of the anions generated in the IRMPD experiments. The substrates ranged from acetylacetone ($\Delta_{acid}H^\circ = 343.8$ kcal mol^{-1}) to 2-cyclohexenone ($\Delta_{acid}H^\circ = 357.5$) and included H_2S, $C_6H_5CH_2CN$, p-cresol, diethyl malonate and acetic acid. Unfortunately, these experiments proved to be difficult for establishing a lower limit for $\Delta_{acid}H^\circ$ because introduction of relatively non-volatile substrates through the pulsed valve was unreliable. Thus, we could not distinguish unequivocally between the acidities of the three primary IRMPD products shown in Eq. (5) and, at best, our experimental results suggest that

$$344 \text{ kcal mol}^{-1} < \Delta_{acid}H^\circ(EtO)_3GeOH, F(EtO)_2GeOH < 350 \text{ kcal mol}^{-1}$$

These results can be compared with the calculated acidities for a number of related species listed in Table 2. While the calculations yield a substantially higher acidity for $F(EtO)_2GeOH$ than for $(EtO)_3GeOH$ it is important to emphasize that the calculated values for the proton affinity of germanate anions relevant to our present study fall close to the range of our experimental results. On the other hand, the calculated proton affinities for the germyl anions proved to be much more sensitive to the level of theory as shown in Table 2 and suggest that different model chemistries may be necessary to assess the correct proton affinities for these species in the absence of reliable experimental values. Further work in this area is presently in progress.

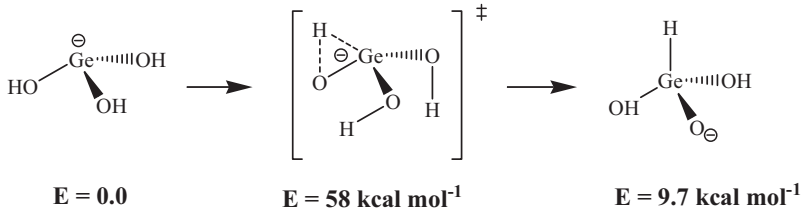

Fig. 4. Mechanism of a germyl–germanate isomerization process with energies and structures calculated at the QCISD(T)/B1//HF/B1 level.

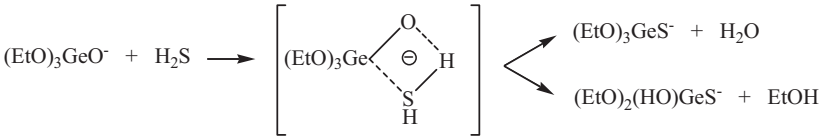

Scheme 2.

Finally, a particularly interesting set of reactions were observed in the bracketing experiments with H_2S and are illustrated below.

$$(EtO)_3GeO^- + H_2S \xrightarrow{56\%} (EtO)_3GeS^- + H_2O \quad (11a)$$

$$(EtO)_3GeO^- + H_2S \xrightarrow{44\%} (EtO)_2(HO)GeS^- + EtOH \quad (11b)$$

$$F(EtO)_2GeO^- + H_2S \xrightarrow{79\%} F(EtO)_2GeS^- + H_2O \quad (12a)$$

$$F(EtO)_2GeO^- + H_2S \xrightarrow{21\%} F(EtO)(HO)GeS^- + EtOH \quad (12b$$

By comparison, no reactions were observed between either $(EtO)_3Ge^-$ or $HGe(OEt)_2^-$ and H_2S, but reactions similar to (11a) and (12a) were observed for $GeFO_2C_2H_4^-$, $GeO_3C_4H_9^-$ and $GeO_3C_2H_5^-$.

These reactions can be visualized to proceed as shown in Scheme 2. While H_2S is less acidic than the corresponding $(EtO)_3GeO^-$, proton abstraction is possible whithin the collision complex to yield $[(EtO)_3GeOH\cdot^-SH]$ as a transient species. This can then proceed by attack of HS^- at the Ge center followed by either H_2O or EtOH elimination. This type of mechanism is possible provided that the proton affinity of the Ge-containing anion does not differ dramatically from that of SH^- (<~10 kcal mol^{-1}) so that the endothermic proton abstraction can be compensated by the stability of the complex.

There are three additional points that are relevant to our discussion: (i) no reactivity with H_2S is observed for the germyl anions $(EtO)_3Ge^-$ and $(EtO)_2GeH^-$ that may reflect very likely a structural difference with the germanate anions in Eqs. (10) and (11) and not a pronounced difference in proton affinities; (ii) the reactivity of the $GeFO_2C_2H_4^-$, $GeO_3C_4H_9^-$ and $GeO_3C_2H_5^-$ with H_2S supports our idea that these ions retain a germanate structure as previously discussed; (iii) formation of these thiogermanate ions is particularly an attractive result because of the important applications of thiogermanate glasses [47] and interest in the synthesis and characterization of thiogermanic acids [48].

5. Conclusions

This work has shown the ease with which pentacoordinated Ge anions can be generated in the gas-phase by reactions of a suitable nucleophile and $Ge(OEt)_4$.

The IRMPD of these $XGe(OEt)_4^-$ species has revealed a sequential set of processes that can give rise to a variety of germyl and germanate anions through what may be loosely described as an "onion-peeling" approach of the hypervalent Ge species. A combination of experimental and theoretical techniques have been used to identify these ions, to estimate their proton-affinities and to establish the fact that oxygen-containing germyl anions are more stable than their isomeric germanolate and germanate structures.

On the basis of these results, further work would be of considerable interest both in characterizing some of these ions spectroscopically and in pursuing studies of the condensation products of germanium alkoxides by electrospray ionization.

Acknowledgments

The authors wish to thank the support of the São Paulo Science Foundation (FAPESP), the Brazilian Research Council (CNPq) and the Air Force Office of Scientific Research (AFOSR). One of us (JMR) also acknowledges the support of the Office of Graduate Education of Brazil (CAPES) for a National Senior Visiting Professorship.

References

[1] J.M. Riveros, Probing the gas-phase ion chemistry of simple Ge systems, Int. J. Mass Spectrom. 221 (2002) 177–190.
[2] R. Damrauer, J.A. Hankin, Chemistry and thermochemistry of silicon-containing anions in the gas-phase, Chem. Rev. 95 (1995) 1137–1160.
[3] H. Basch, Bond dissociation energies in organometallic compounds, Inorg. Chim. Acata 252 (1996) 265–279.
[4] P. Serp, P. Kalck, R. Feurer, Chemical vapor deposition methods for the controlled preparation of supported catalytic materials, Chem. Rev. 102 (2002) 3085–3128.
[5] D.C. Bradley, Metal alkoxides as precursors for electronic and ceramic materials, Chem. Rev. 89 (1989) 1317.
[6] J.L. Lensch-Falk, E.R. Hemesath, F.J. Lopez, L.J. Lauhon, Vapor–solid–solid synthesis of ge nanowires from vapor-phase-deposited manganese germanide seeds, J. Am. Chem. Soc. 129 (2007) 10670–10671.
[7] K.K. Kalebaila, D.G. Georgiev, S.L. Brock, Synthesis and characterization of germanium sulfide aerogels, J. Non-Cryst. Solids 352 (2006) 232–240.
[8] J.D. Rimer, D.D. Roth, D.G. Vlachos, R.F. Lobo, Self-assembly and phase behavior of germanium oxide nanoparticles in basic aqueous solutions, Langmuir 23 (2007) 2784–2791.
[9] T.M. Davis, M.A. Snyder, M. Tsapatsis, Germania nanoparticles and nanocrystals at room temperature in water and aqueous lysine sols, Langmuir 23 (2007) 12469–12472.
[10] K. Okumura, K. Asakura, Y. Iwasawa, Characterization of GeO_2 sub-monolayers on SiO_2 prepared by chemical vapor deposition of $Ge(OMe)_4$ by EXAFS, FT-IR, and XRD, Langmuir 14 (1998) 3607–3613.
[11] J. Pola, R. Fajgar, Z. Bastl, L. Diaz, Chemical vapor deposition of reactive organogermanium films by laser-induced decomposition of tetramethoxygermane, J. Mater. Chem. 2 (1992) 961–964.
[12] T.N.M. Bernards, E.W.J.L. Oomen, M.J. Vanbommel, A.H. Boonstra, The effect of TEOG on the hydrolysis-condensation mechanism of a two-step sol–gel process of TEOS, J. Non-Cryst. Solids 142 (1992) 215–224.
[13] T.N.M. Bernards, M.J. Vanbommel, E.W.J.L. Oomen, A.H. Boonstra, Hydrolysis-condensation mechanism of a two-step sol–gel process of mixtures of TEOS and TEOG, J. Non-Cryst. Solids 147/148 (1992) 13–17.
[14] V. Krishnan, S. Gross, S. Müller, L. Armelao, E. Tondello, H. Bertagnolli, Structural investigations on the hydrolysis and condensation behavior of pure and chemically modified alkoxides. 2. Germanium alkoxides, J. Phys. Chem. B 111 (2007) 7519–7528.

[15] J. Beckmann, K. Jurkschat, M. Schürman, On the hydrolysis of $tBu_2Ge(OEt)_2$: supramolecular self assembly in the solid state of 2 $tBu_2Ge(OH)_2$, $(tBu_2GeOH)_2O$ and H_2O, Eur. J. Inorg. Chem. (2000) 939–941.
[16] J.R.T. Johnson, I. Panas, Structure, bonding and formation of molecular germanium oxides, hydroxides and oxyhydroxides, Chem. Phys. 249 (1999) 273–303.
[17] S. Cristoni, L. Armelao, S. Gross, R. Seraglia, E. Tondello, P. Taldi, Study of polycondensation reactions of $Ge(OEt)_4$ and $Ge(OEt)_4/Si(OEt)_4$ by electrospray ionization mass spectrometry, Rapid Commun. Mass Spectrom. 16 (2002) 733–737.
[18] S. Zink, T. Eichner, M. Schnell, J. Woenckhaus, Electrospray mass spectra of oligo germanium acids and oligo chloro germanium acids appearing during germanium tetra-ethoxide hydrolisation, Z. Phys. Chem. (Muenchen, Ger.) 219 (2005) 1355–1371.
[19] B.B. Schaack, W. Schrader, F. Schüth, Detection of structural elements of different zeolites in nucleating solutions by electrospray ionization mass spectrometry, Angew. Chem. Int. Ed. 47 (2008) 9092–9095.
[20] L.A. Xavier, J.M. Riveros, Gas-phase ion chemistry of $Ge(OCH_3)_4$, Int. J. Mass Spectrom. 179/180 (1998) 223–230.
[21] N.H. Morgon, L.A. Xavier, J.M. Riveros, Gas-phase nucleophilic reactions of $Ge(OCH_3)_4$: experimental and computational characterization of pentacoordinated Ge anions, Int. J. Mass Spectrom. 195/196 (2000) 363–375.
[22] L.A. Xavier, J.M. Riveros, Gas-phase ion chemistry of $Ti(O\text{-}i\text{-}Pr)_4$, Can. J. Chem. 83 (2005) 1913–1920.
[23] O.H. Johnson, H.E. Fritz, Tetralkoxygermanes, J. Am. Chem. Soc. 75 (1953) 718–720.
[24] D.S. Tonner, T.B. McMahon, Consecutive infrared multiphoton dissociations in a fourier transform ion cyclotron resonance mass spectrometer, Anal. Chem. 69 (1997) 4735–4740.
[25] J.W. Gauthier, T.R. Trautman, D.B. Jacobson, Sustained off-resonance irradiation for collision-activated dissociation involving Fourier transform mass spectrometry. Collision-activated dissociation technique that emulates infrared multiphoton dissociation, Anal. Chim. Acta 246 (1991) 211–225.
[26] M.J. Frisch, G.W. Trucks, H.B. Schlegel, G.E. Scuseria, M.A. Robb, J.R. Cheeseman, J.A. Montgomery, Jr, T. Vreven, K.N. Kudin, J.C. Burant, J.M. Millam, S.S. Iyengar, J. Tomasi, V. Barone, B. Mennucci, M. Cossi, G. Scalmani, N. Rega, G.A. Petersson, H. Nakatsuji, M. Hada, M. Ehara, K. Toyota, R. Fukuda, J. Hasegawa, M. Ishida, T. Nakajima, Y. Honda, O. Kitao, H. Nakai, M. Klene, X. Li, J.E. Knox, H.P. Hratchian, J.B. Cross, V. Bakken, C. Adamo, J. Jaramillo, R. Gomperts, R.E. Stratmann, O. Yazyev, A.J. Austin, R. Cammi, C. Pomelli, J.W. Ochterski, P.Y. Ayala, K. Morokuma, G.A. Voth, P. Salvador, J.J. Dannenberg, V.G. Zakrzewski, S. Dapprich, A.D. Daniels, M.C. Strain, O. Farkas, D.K. Malick, A.D. Rabuck, K. Raghavachari, J. B. Foresman, J. V. Ortiz, Q. Cui, A. G. Baboul, S. Clifford, J. Cioslowski, B. B. Stefanov, G. Liu, A. Liashenko, P. Piskorz, I. Komaromi, R.L. Martin, D.J. Fox, T. Keith, M.A. Al-Laham, C.Y. Peng, A. Nanayakkara, M. Challacombe, P.M.W. Gill, B. Johnson, W. Chen, M.W. Wong, C. Gonzalez, J.A. Pople, Gaussian 03, Revision D.01, Gaussian, Inc., Wallingford CT, 2004.
[27] M.P. Andersson, P. Uvdal, New scale factors for harmonic vibrational frequencies using the B3LYP density functional method with the triple-ζ basis set 6-311+G(d,p), J. Phys. Chem. A 109 (2005) 2937–2941.
[28] N.H. Morgon, J.M. Riveros, Electron affinity of $X_nGe(OMe)_{3-n}$ radicals (X = H, F; n = 0–2) and the Ge–H bond dissociation energy, Int. J. Mass Spectrom. A 210/211 (2001) 173–180.
[29] L.A. Xavier, N.H. Morgon, J.J. Menegon, J.M. Riveros, Photodetachment of $FSi(OMe)_4^-$ and $FGe(OMe)_4^-$ anions: an experimental and theoretical study of gas-phase hypervalent Si and Ge species, Int. J. Mass Spectrom. 219 (2002) 485–495.
[30] C. Hao, J.D. Kaspar, C.E. Check, K.C. Lobring, T.M. Gilbert, L.S. Sunderlin, Effect of substituents on the strength of A–Cl^- (A = Si, Ge, and Sn) bonds in hypervalent systems ACl_5^-, ACl_4F^-, and $A(CH_3)_3Cl_2^-$, J. Phys. Chem. A 109 (2005) 2026–2034.
[31] S.A. McLuckey, D.M. Goeringer, Slow heating methods in tandem mass spectrometry, J. Mass Spectrom. 32 (1997) 461–474.
[32] K. Mochida, H. Suzuki, M. Nanba, T. Kugita, Y. Yokoyama, Generation and reactions of metal-free trialkyl germyl anions from silylgermane and digermane, J. Organometal. Chem. 499 (1995) 83–88.
[33] Y. Yokoyama, K. Mochida, Stereoselective syntheses of 2-fluoro-2-methyl-3-hydroxypropionamides by use of a germyl anion species, Synlett (1998) 37–38.
[34] H.R. Kricheldorf, S. Rost, Spyrocycles versus networks: polycondensation of $Ge(OEt)_4$ with various aliphatic α,ω-diols, Macromolecules 37 (2004) 7955–7959.
[35] E. Bonefille, S. Mazieres, C. Bibal, N. Saffon, H. Gornitzka, C. Couret, A synthetic equivalent of a germanone derivative, Eur. J. Inorg. Chem. (2008) 4242–4247.
[36] R. Withnall, L. Andrews, Matrix reactions of germane and oxygen atoms. Infrared spectroscopic evidence for germylene–water complex, germanone, germanol, hydroxygermylene, and germanic acid, J. Phys. Chem. 94 (1990) 2351–2357.
[37] S.P. So, Ab initio molecular orbital study of the reaction of GeH_2 with H_2O and decomposition reactions of H_3GeOH, J. Phys. Chem. A 105 (2001) 4988–4991.
[38] M.L.P. da Silva, J.M. Riveros, Gas-phase nucleophilic reactions in tetraalkoxysilanes, J. Mass Spectrom. 30 (1995) 733–740.
[39] C.H. DePuy, V.M. Bierbaum, L.A. Flippin, J.J. Grabowski, G.K. King, R.J. Schmitt, S.A. Sullivan, Gas-phase reactions of anions with substituted silanes, J. Am. Chem. Soc. 102 (1980) 5012–5015.
[40] I.H. Krouse, P.G. Wenthold, Fluorotrimethylsilane affinities of anionic nucleophiles: a study of fluoride-induced desilylation, J. Am. Soc. Mass Spectrom. 16 (2005) 697–707.
[41] J.A. Tossell, N. Sahai, Calculating the acidity of silanols and related oxyacids in aqueous solution, Geochim. Chosmochim. Acta 64 (2000) 4097–4113.
[42] G.S. Pokrovski, J. Schott, Thermodynamic properties of aqueous Ge(IV) hydroxide complexes from 25 to 350 °C: Implications for the behavior of germanium and the Ge/Si ratio in hydrothermal fluids, Geochim. Chosmochim. Acta 62 (1998) 1631–1642.
[43] J.-F. Boily, AIM and ELF analyses and gas-phase acidities of some main-group oxyacids (H_2XO_4, X = Cl, S, P, Si and Br, Se, As, Ge), J. Phys. Chem. A 107 (2003) 4276–4285.
[44] M. Decouzon, J.F. Gal, J. Gayraud, P.C. Maria, G.A. Vaglio, P. Volpe, Fourier transform-ion cyclotron resonance study of the gas-phase acidities of germane and methylgermane; bond dissociation energy of germane, J. Am. Soc. Mass Spectrom. 4 (1993) 54–57.
[45] N.H. Morgon, J.M. Riveros, Calculation of the proton and electron affinity of simple Ge-containing species using density functional theory, J. Phys. Chem. A 102 (1998) 10339–10403.
[46] J. Bartmess, NIST Chemistry WebBook, NIST Standard Reference Database Number 69, National Institute of Standards and Technology, Gaithersburg, MD, 20899.
[47] R.J. Curry, A.K. Mairaj, C.C. Huang, R.W. Eason, C. Grivas, D.W. Hewak, J.V. Badding, Chalcogenide glass thin films and planar waveguides, J. Am Ceram. Soc. 88 (2005) 2451–2455.
[48] S.A. Poling, C.R. Nelson, J.T. Sutherland, S.W. Martin, Synthesis and characterization of the thiogermanic acids $H_4Ge_4S_{10}$ and $H_2Ge_4S_9$, J. Phys. Chem. B 107 (2003) 5413–5418.